ChemComm

# Sulfonic-acid-based lyotropic bicontinuous cubic polymer network for molecular-size-selective heterogeneous catalysis



| | |
|---|---|
| Journal: | *ChemComm* |
| Manuscript ID | CC-COM-06-2023-002653.R2 |
| Article Type: | Communication |
| | |

COMMUNICATION

# Sulfonic-acid-based lyotropic bicontinuous cubic polymer network for molecular-size-selective heterogeneous catalysis†

Received 00th January 20xx,
Accepted 00th January 20xx

DOI: 10.1039/x0xx00000x

Keira E. Culley,[a] Christopher Johnson[b] and Douglas L. Gin*[a]

**A nanoporous, bicontinuous cubic, lyotropic liquid crystal polymer resin with sulfonic acid groups is presented that exhibits high catalytic activity and is capable of molecular-size-selective heterogeneous acid catalysis.**

Molecular-size-selective heterogeneous catalysts are important in organic chemistry and chemical industry. Facile catalyst recovery/recyclability and high reaction selectivity are essential for low-cost and efficient reaction processes.[1] Generally, these catalysts are solid materials with nanometer-scale pores that provide the desired selectivity via molecular size-exclusion. The most prevalent examples of such catalysts – zeolites, metal-organic frameworks (MOFs), and covalent-organic frameworks (COFs) – are highly crystalline and suffer from shortcomings such as brittleness and poor processability.[2-4] Inorganic zeolites have uniform, angstrom-scale pores that provide excellent molecular selectivity; however, many MOFs and COFs have relatively large nanopores which reduce selectivity.[3,4] In addition, some of these latter materials rely on precious or transition metals to form the catalytic sites, making them more expensive and less environmentally benign.[3,4]

Catalytic lyotropic liquid crystal (LLC) polymer resins are a relatively new class of molecular-size-selective heterogeneous catalysts that are formed by the phase separation (upon addition of a polar solvent) of amphiphilic monomers containing catalytic headgroups, followed by in-situ cross-linking to lock-in the formed periodic, nanoporous mesophases.[5] Catalytic LLC resins have several benefits and distinctive properties compared to the other types of heterogeneous catalysts mentioned previously: Unlike the larger pores often created in COFs and MOFs, LLC networks have monodisperse nanopores on the scale of single molecules (*i.e.,* ca. 1 nm or smaller),[6] resulting in high size selectivity. They also have enhanced reactivity due to high catalytic site density since the pore walls are completely lined by the amphiphile headgroups as a result of the LLC self-assembly process.[6] Different catalytic groups can also be incorporated into LLC pores, and pore size can be modified via design of the starting monomers.[6] Finally, prior to cross-linking, these materials can be processed to form flexible, defect-free, thin polymer films and other form factors.[6]

Our research group has previously designed several catalytic LLC resins that perform Brønsted base, Lewis acid, Brønsted acid, and mild oxidative catalysis.[7-10] These initial catalysts were all based on the inverted hexagonal ($H_{II}$) LLC phase, which has close-packed, 1-D cylindrical nanopores. Although the catalytic performance of these LLC resins was enhanced compared to non-ordered catalyst resins due to their uniform, ordered nanostructure, the $H_{II}$ phase is not the best phase architecture for uptake, reactive site access, or transport applications.[11] This is because the 1-D pores can be easily blocked or misaligned in a sample. High throughput and good pore access require the $H_{II}$ pores to be aligned and continuous throughout the sample.

In contrast, bicontinuous cubic (Q) LLC phases possess 3D-interconnected nanopore systems with overall cubic symmetry that do not require macroscopic pore alignment for good transport or access.[11,12] A Q-phase network with catalytically active, hydrophilic headgroups would have higher accessibility to the catalyst sites compared to lower-dimensionality LLC phases, such as the 1-D hexagonal (H) and 2-D lamellar (L) phases. Q-phase polymers have been used as drug delivery materials and filtration membranes;[13,14] however, they have not been utilized for catalysis yet. This is because Q phases are typically very sensitive to amphiphile structure and environment, requiring specific amphiphile motifs and precise amphiphile/solvent compositions in order to form.[15] There is currently only one report of a Q-phase network with added functional properties.[15] This stimuli-responsive material was only able to be formed by blending a non-Q-phase-forming monomer containing a functional headgroup with a known Q-phase monomer system.[15] To date, no catalytic Q-phase polymer networks have been reported.

Herein, we present the development of a nanoporous Q-

[a] *Department of Chemistry, University of Colorado, Boulder, CO 80309, USA.*
[b] *Department of Chemical and Biomolecular Engineering, University of Pennsylvania, Philadelphia, PA 19104, USA.*

† Electronic Supplementary Information (ESI) available: synthetic procedures, analytical data on materials, catalysis reaction procedures and data, and structure calculations. See DOI: 10.1039/x0xx00000x

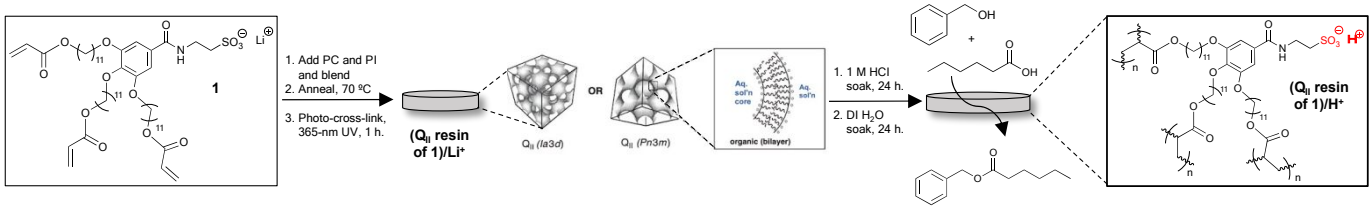


**Fig. 1** $Q_{II}$ phase formation and cross-linking of **1** to form the **($Q_{II}$ resin of 1)/$Li^+$**, $H^+$ for $Li^+$ ion exchange to form the **($Q_{II}$ resin of 1)/$H^+$**, and its resulting catalytic activity.

phase LLC polymer resin with sulfonic-acid groups that is capable of molecular-size-selective heterogeneous acid catalysis. This material was prepared by postpolymerisation $H^+$ for $Li^+$ cation exchange of a $Q_{II}$-phase polymer resin (**($Q_{II}$ resin of 1)/$Li^+$**) (Fig. 1) made from a previously reported lithium sulfonate monomer (**1**).[16] The resulting new acid-exchanged $Q_{II}$-phase resin (**($Q_{II}$ resin of 1)/$H^+$**) (Fig. 1) was tested as catalyst particles in the esterification test reaction of 1-hexanoic acid with various benzyl alcohol (BA) derivatives (Fig. 2). The **($Q_{II}$ resin of 1)/$H^+$** exhibited high molecular-size-selectivity: BA derivatives with molecular diameters ≥1.68 nm were rejected almost entirely with little-to-no catalytic activity (*i.e.*, 2% conversion), while BA derivatives with molecular diameters ≤1.25 nm passed through the pores and reacted at significantly higher rates (*i.e.*, 87% conversion). The **($Q_{II}$ resin of 1)/$H^+$** can also be recycled with retention of greater than 90% conversion after three rounds of reuse. To our knowledge, a catalytic Q-phase resin with these capabilities is unprecedented.

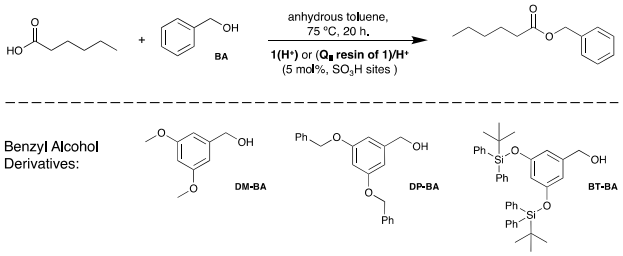


**Fig. 2** Esterification reaction used for heterogeneous catalyst testing with different-size derivatives of BA.

For design and demonstration of an initial Q-phase LLC catalyst resin, sulfonic-acid catalysis was chosen as a test platform for three reasons: First, Brønsted acid catalysis is one of the most widely used forms of catalysis industrially, and there are a number of commercial, amorphous, sulfonic-acid resins available for comparison.[9] Second, prior work in our group showed that this type of catalysis was successful using an $H_{II}$ resin, where the uniform nanoporous structure generated higher reaction selectivity compared to amorphous sulfonic-acid resins.[9] Third, a sulfonic-acid Q-phase resin can be easily prepared in one step (*i.e.*, ion exchange) from a $Q_{II}$-phase Li salt resin that was previously made by our group from monomer **1** and used for enhanced Li ion transport.[16]

Unfortunately, it was not possible to prepare a sulfonic-acid $Q_{II}$ resin directly from the corresponding acid derivative of this LLC monomer (*i.e.*, **1($H^+$)**), even though the single-head/three-tail ionic amphiphile motif has been found to form $H_{II}$ and $Q_{II}$ phases.[9,10,16] Although monomer **1($H^+$)** was successfully synthesized and purified, it did not form a Q phase when tested with a number of added polar solvents. The $Li^+$ cation in the headgroup of this monomer platform was found to be necessary to induce self-assembly into a Q phase.[16] As stated previously, modifications to known Q-phase monomers often result in the loss of the ability to form a Q phase due to the extreme sensitivity of the phase.[15] Doping or blending **1($H^+$)** with another $Q_{II}$-phase-forming monomer to form a $Q_{II}$ phase was not preferred because of the inherent decrease in catalytic site density in the LLC pores as a result of dilution with a non-catalytic monomer. Consequently, a sulfonic-acid Q-phase LLC catalyst test resin was prepared by acid exchange of a $Li^+$ salt $Q_{II}$-phase resin made from **1.**

This acidic $Q_{II}$-phase resin was prepared as follows: A bulk film of **($Q_{II}$ resin of 1)/$Li^+$** was first prepared by photo-cross-linking a $Q_{II}$ mixture of monomer **1** containing 15 wt% propylene carbonate (PC) and 1 wt% radical photo-initiator (PI) as previously described (see the ESI†, Section IV).[16] As shown in Fig. 3, the $Q_{II}$ phase in the initial **($Q_{II}$ resin of 1)/$Li^+$**) film was confirmed by polarized light microscopy (PLM) (*i.e.*, the presence of a black optical texture) and small-angle X-ray scattering (SAXS) (*i.e.*, a SAXS profile with a $q$-spacing ratio of $q^*$ $A^{-1}$, $\sqrt{2}q^*$ $A^{-1}$, and $\sqrt{3}q^*$ $A^{-1}$) (see ESI†, Section IV for details).[15] Prior work confirmed that this Q phase was a type II (*i.e.*, reverse) phase due to an observed L phase at higher PC content.[16] This Li-salt bulk film was then soaked in 1 M aq. HCl for 24 h at RT to perform $Li^+$ for $H^+$ exchange. $Q_{II}$ phase retention in the resulting acidified **($Q_{II}$ resin of 1)/$H^+$** film was confirmed by PLM and SAXS, as mentioned previously (see Fig. 3). Only a trace amount of Li in the acidified material was detected by elemental analysis. The **($Q_{II}$ resin of 1)/$H^+$** film was then ground into a powder and sieved to select the 75–150 μm particles to increase and normalize resin surface area for heterogeneous catalysis.[7-10] $Q_{II}$ phase retention was confirmed again via SAXS. BET gas adsorption analysis cannot be used to characterize the pores and surface area of LLC resins because of the inability to completely remove solvent from the nanopores (see ESI†, Section IV for full acid resin characterisation details).

The reaction selected for acid catalysis testing was the esterification of various BA derivatives with 1-hexanoic acid (Fig. 2). This reaction employing just BA as the starting alcohol was previously used to compare the catalytic performance of an $H_{II}$ sulfonic-acid resin against that of amorphous, commercial acid resins.[9] However, in the present study, a series of increasingly sized BA derivatives were tested under the same reaction conditions to determine the effective pore size of the **($Q_{II}$ resin of 1)/$H^+$** by observing the onset of molecular-size rejection (*i.e.*, substrates larger than the pores will not be able to enter and be catalysed for reaction). Specifically, the

 

following BA derivatives (with their calculated molecular diameters) were used: BA (0.69 nm), 3,5-dimethylbenzyl alcohol (DM-BA, 0.98 nm), 3,5-bis(benzyloxy)benzyl alcohol (DP-BA, 1.25 nm), and 3,5-bis(*tert*-butyldiphenylsilyoxy)benzyl alcohol (BT-BA, 1.68 nm) (see the ESI†, Section V). We found that using equimolar amounts of these BA derivatives and 1-hexanoic acid (0.25 M) in the presence of the **($Q_{II}$ resin of 1)/$H^+$** (5 mol% $SO_3H$ sites relative to the reactants based on resin composition) with anhydrous toluene as the reaction solvent at 75 °C allowed for significant conversion of the starting materials in 20 h.

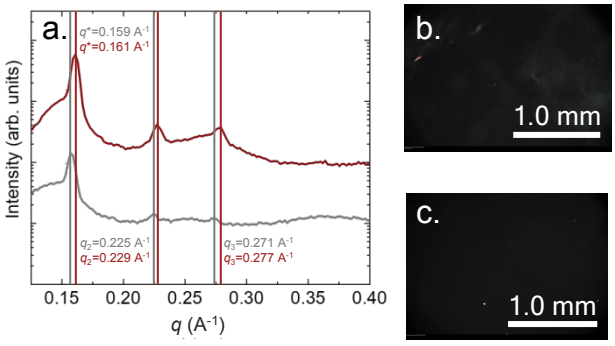


**Fig. 3** (a) SAXS spectra of the **($Q_{II}$ resin of 1)/$Li^+$** (red line) and of the **($Q_{II}$ resin of 1)/$H^+$** (grey line) sample produced after $H^+$ for $Li^+$ exchange. PLM images of the materials (mag = 50x): (b) before acidification and (c) after acidification.

Under these conditions, control reactions with no added acid catalyst showed zero conversion of BA to the ester product in 20 h by $^1$H-NMR analysis (see Table 1, entry A). Solution-phase catalysis tests using unpolymerised monomer **1($H^+$)** (5 mol% $SO_3H$ sites relative to the reactants) afforded (87 ± 7)% conversion of BA to the expected ester in 20 h (see Table 1, entry B). The larger BA derivatives – DM-BA, DP-BA, and BT-BA – also demonstrated similar significant conversion values with the **1($H^+$)** solution-state catalyst (see the ESI†, Table S2). These findings indicate that each BA derivative tested reacts similarly (and to high conversion) with the solution-state acid catalyst, so any observed differences in reaction rate (*i.e.*, size selectivity) with the solid-state **($Q_{II}$ resin of 1)/$H^+$** should be due to the uniform-size $Q_{II}$ nanopores.

Use of the **($Q_{II}$ resin of 1)/$H^+$** as a heterogeneous catalyst (5 mol% loading based on $SO_3H$ sites) retained high conversion of BA, DM-BA, and DP-BA over the same 20-h reaction time; however, BT-BA (the largest BA derivative, 1.68 nm) showed little-to-no conversion even after 163 h. (Fig. 4a). As seen in Fig. 4b, BA, DM-BA, and DP-BA all exhibit a similar drop in total conversion after 20 h of reaction for the heterogeneous reactions compared to the solution-state reactions, likely due to similar diffusion times into the nanopores. However, the conversion of BT-BA for the heterogenous reaction drops off almost completely compared to the solution-state case. The small (2 ± 1)% conversion of BT-BA observed with the **($Q_{II}$ resin of 1)/$H^+$** after 20 h is likely not due to BT-BA entry into the pores but rather due to surface catalysis from the few $SO_3H$ sites on the surface of the resin particles (Table 1, entry E).[9] This conclusion is supported by the fact that when the % conversion of BT-BA for the heterogenous reaction is monitored as a function of time (Fig. 4a), it did not continue to increase with time, as for the other BA derivatives. This continued increase in conversion over time for BA, DM-BA, and DP-BA is indicative of a slow diffusion rate into the nanopores, followed by heightened reactivity once inside.[17] In contrast, BT-BA does not appear to enter the catalytic pores at all, presumably due to pore size rejection. Instead, it only reacts at a very low rate via the small amount of surface $SO_3H$ sites on the resin. Based on the calculated diameters of the BA derivatives tested (see ESI†, Section V), these heterogeneous catalysis results suggest that the nanopores in the **($Q_{II}$ resin of 1)/$H^+$** are between 1.25 nm and 1.68 nm in diameter.

**Table 1** Summary of substrate conversion and selectivity (BA/BT-BA) with various acid catalysts. Reaction conditions: 5 mol% catalytic $SO_3H$ sites relative to reactants, anh. toluene solvent, 75 °C, 20 h. Avg values over 3 indep. runs with std. dev. error bars.

| Entry | Catalyst | BA conversion in 20 h (%) | BT-BA conversion in 20 h (%) | Molar selectivity (BA/BT-BA) |
|---|---|---|---|---|
| A | None | Not detected | Not detected | n/a |
| B | **1($H^+$)** (soln) | 87 ± 7 | 38 ± 5 | 2.4 ± 0.1 |
| C | **(Mixed-phase resin of 1)/$H^+$** | 58 ± 2 | 56 ± 1 | 1.03 ± 0.01 |
| D | Dowex® resin | 30 ± 3 | Not detected | n/a |
| E | **($Q_{II}$ resin of 1)/$H^+$** | 60 ± 5 | 2 ± 1 | 27 ± 5 |

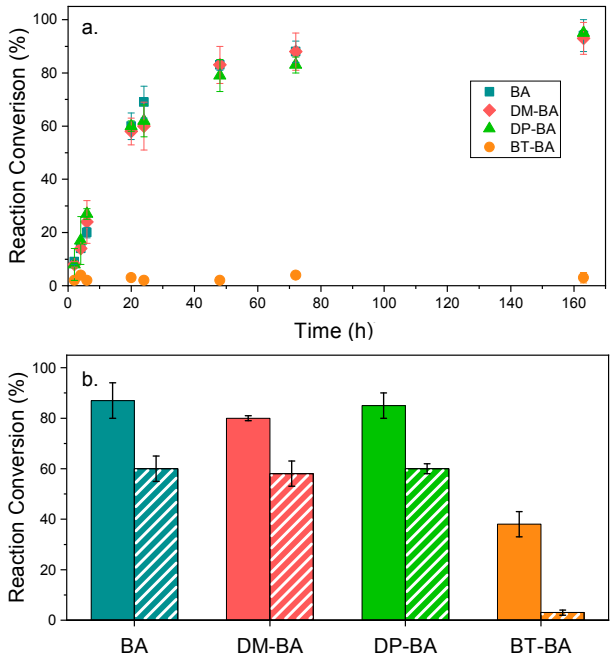


**Fig. 4** (a) Percent conversion as a function of time for reaction of the BA derivatives with 1-hexanoic acid using **($Q_{II}$ resin of 1)/$H^+$** as a solid catalyst (5 mol% $SO_3H$ sites relative to reactants based on resin composition. (b) Percent conversion of the BA derivatives with 1-hexanoic acid after 20 h at 75 °C with 5 mol% monomer **1($H^+$)** as a solution acid catalyst (solid bars) and with solid **($Q_{II}$ resin of 1)/$H^+$** (5 mol% $SO_3H$ sites relative to reactants) (striped bars). Values shown are avg values over 3 indep. runs with std. dev. error bars.

The large difference between solution-state catalysis with monomer **1($H^+$)** and heterogeneous catalysis with the **($Q_{II}$ resin of 1)/$H^+$** can be seen in the reaction selectivity for BA vs. BT-BA in Table 1 as a figure of merit (*i.e.*, (2.4 ± 0.1) vs. (27 ± 5) (mol/mol) BA/BT-BA, respectively). For simplicity, only the BA/BT-BA selectivity is shown in Table 1; however, the DM-

BA/BT-BA and DP-BA/BT-BA values are nearly identical to the BA/BT-BA values for both the solution- and solid-state reactions (see ESI†, Table S3). These results support the presence of a threshold pore size in the $Q_{II}$ acid resin: When the molecular diameter of the reacting alcohol is less than that of the $Q_{II}$ pores, reactivity is high and similar due to facile entry to the catalytic pores. However, when the diameter of the BA derivative is larger than the pores, appreciable catalysis does not occur due to the inability to enter the pores. These results also suggest that the **($Q_{II}$ resin of 1)/$H^+$** retains high catalytic activity due to the high density of acid sites lining the pores.

To confirm that the high substrate selectivity was due to the uniform-size nanopores in the $Q_{II}$-phase nanostructure, the same esterification test reaction was performed with a mixed-phase LLC acid control resin prepared by cross-linking monomer **1** at RT with no added PC and then acidifying. (It was not possible to form an LLC acid resin with exactly the same composition as the **($Q_{II}$ resin of 1)/$H^+$** because the starting **1** + PC mixture did not change phase even with extended temperature changes (see the ESI†, Section IV)). The esterification test reactions catalysed by the **(mixed-phase resin of 1)/$H^+$** gave an average reaction conversion of (58 ± 2)% for BA and (56 ± 1)% for BT-BA over 20 h, with a BA/BT-BA selectivity of only 1.03 ± 0.01 (Table 1, entry C). This very low selectivity between the smallest and the largest BA derivatives demonstrates that the lack of a uniform nanoporous structure decreases the molecular-size-selectivity of the solid catalyst.

The recyclability of the **($Q_{II}$ resin of 1)/$H^+$** was also investigated over three consecutive trials of the esterification of BA with 1-hexanoic acid. It was found that this catalyst can be reused with only a slight loss in both catalyst recovery and catalytic activity (see ESI†, pp S16–S17).

Finally, the catalytic activity and substrate selectivity of the **($Q_{II}$ resin of 1)/$H^+$** was compared to a commercial, amorphous, sulfonic-acid resin: Dowex® 50WX4-100, $H^+$ form (a gel-type resin) (see ESI†, pp S17–S18 for details). As shown in Table 1, both the Dowex® resin and the **($Q_{II}$ resin of 1)/$H^+$** did not catalyse the reaction of large BT-BA but only the smaller BA derivatives. However, under identical reaction conditions, the **($Q_{II}$ resin of 1)/$H^+$** was far more catalytically active for the reaction of BA than the Dowex® resin (see Table 1, entry D). The former was also far more selective in producing the desired ester product (ester/ether molar selectivity: (6.1 ± 0.5) x $10^3$), whereas Dowex® produced a mixture of products including dibenzyl ether (ester/ether selectivity: 0.6 ± 0.1) (see ESI†, Fig. S13). As mentioned in an earlier paper, formation of significant ether side product vs. the desired ester for this test reaction can be attributed to the presence of non-uniform-size pores with different acid strengths that can generate alternate products.[9] Our current results confirm the importance of the nanoporous Q-phase structure on the molecular-size selectivity and reactivity of the catalyst resin.

In summary, we have demonstrated the first example of a catalytically active $Q_{II}$-phase polymer network. This sulfonic-acid-based LLC resin exhibits high catalytic activity and excellent molecular-size selectivity via exclusion of reactants above a certain size from the LLC nanopores. Esterification reaction testing with different-size BA derivatives indicated an effective pore size of between 1.25 and 1.68 nm for the $Q_{II}$ resin. This nanoporous acid resin also showed much higher activity and reactant size selectivity compared to a commercial, amorphous, sulfonic-acid resin. Future work will focus on (1) exploring if the pore size of this $Q_{II}$ resin can be controlled via monomer or phase composition modification; (2) determining its pore size more accurately via TEM imaging; and (3) demonstrating size-selective catalysis in a flow-through membrane format to separate reactants and products of different sizes. We also plan to more thoroughly compare this Q-phase resin against compositionally similar LLC acid resins with other nanostructures to demonstrate its benefits in catalysis.

K. E. C and D. L. G. thank the Army Research Office for partial funding through STTR subcontract grants with TDA Research, Inc. (W911NF-21-C-0027 and W911NF-22-C-0012). C. J. thanks the National Science Foundation (DMR-1720530) for partial funding of the SAXS instrument used at the Univ. of Pennsylvania, and acknowledges that the work performed was funded in part by the Vagelos Institute of Energy Science and Technology at the Univ. of Pennsylvania.

## Conflicts of interest

There are no conflicts to declare.

## References

1 S. M. George, *Chem. Rev.*, 1995, **95**, 475–476.
2 Y. Li and J. Yu, *Nat. Rev. Mater.*, 2021, **6**, 1156–1174.
3 X. Ma, F. Liu, Y. Helian, C. Li, Z. Wu, H. Li, H. Chu, Y. Wang, Y. Wang, W. Lu, M. Y. Guo and S. Zhou, *Energy Convers. Manag.*, 2021, **229**, 113760.
4 H. Hu, Q. Yan, R. Ge and Y. Gao, *Chin. J. Catal.*, 2018, **39**, 1167–1179.
5 Y. Saadat, O. Q. Imran and C. O. Osuji, *J. Mater. Chem. A*, 2021, **9**, 21607–21658.
6 D. L. Gin, C. S. Pecinovsky, J. E. Bara and R. L Kerr, *Struct. Bond.*, 2008, **128**, 181–222.
7 S. A. Miller, E. Kim, D. H. Gray and D. L. Gin, *Angew. Chem. Int. Ed.,* 1999, **38**, 3021–3026.
8 W. Gu, W. J. Zhou and D. L. Gin, *Chem. Mater.*, 2001, **13**, 1949–1951.
9 Y. Xu, W. Gu and D. L. Gin, *J. Am. Chem. Soc.*, 2004, **126**, 1616–1617.
10 G. E. Dwulet and D. L. Gin, *Chem. Commun.*, 2018, **54**, 12053–12056.
11 B. R. Wiesenauer and D. L. Gin, *Polym. J.*, 2012, **44**, 461.
12 O. Q. Imran, P. Li, N. K. Kim, D. L. Gin and C. O. Osuji, *Chem. Commun.*, 2021, **57**, 10931–10934.
13 S. V. Rao, B. N. Sravya and K. Padmalatha, *GSC Biol. Pharm. Sci.*, 2018, **5**, 76–81.
14 B. M. Carter, B. R. Wiesenauer, R. D. Noble and D. L. Gin, *J. Membr. Sci.*, 2014, **455**, 143–151.
15 P. Li, C. Johnson, S. S. Dyer, C. O. Osuji and D. L. Gin, *Adv. Mater. Interfaces*, 2023, **10**, 2201761.
16 R. L. Kerr, R. K. Shoemaker, B. J. Elliott and D. L. Gin, *J. Am. Chem. Soc.*, 2009, **131**, 15972–15973.
17 S. Sahu, N. S. Schwindt, B. J. Coscia and M. R. Shirts, *J. Phys. Chem. B.*, 2022, **126**, 10098–10110.